ELSEVIER

Journal of Biomechanics 40 (2007) 1988–1994

JOURNAL OF BIOMECHANICS

www.elsevier.com/locate/jbiomech
www.JBiomech.com

Combined experimental and numerical analysis of the flow structure into the left ventricle

F. Domenichini[a,*], G. Querzoli[b], A. Cenedese[c], G. Pedrizzetti[d]

[a]*Dipartimento di Ingegneria Civile, University of Firenze, Italy*
[b]*Dipartimento di Ingegneria del Territorio, University of Cagliari, Italy*
[c]*Dipartimento di Idraulica, Trasporti e Strade, University of Roma La Sapienza, Italy*
[d]*Dipartimento di Ingegneria Civile e Ambientale, University of Trieste, Italy*

Accepted 18 September 2006

Abstract

Fluid dynamics is used for diagnosis in cardiology only to a partial extent. Indeed several aspects of cardiac flows and their relation with pathophysiology are unknown. The flow that develops into the left ventricle is here studied by using a combination of numerical and experimental models. The former allows a detailed three-dimensional analysis, the latter can be used in conditions, like in presence of turbulence, that are out of reach of the current computational power. The three-dimensional flow dynamics is analyzed in terms of its vortical structure. The study, within its limitations, provides further physical understanding about the intraventricular flow structure. This could eventually support the development of cardiac diagnostic indicators based on fluid dynamics.

Keywords: Left ventricle; Fluid dynamics; Turbulence; Experimental method; Numerical simulation

1. Introduction

In the last years, the technological advances have permitted the development of diagnostic tools (magnetic resonance imaging, ultrasound, computed tomography) that produce an enormous amount of data about the cardiac structure and function. These data are mostly used for visualization purposes, although physically-based models would be required in order to improve their interpretation and eventually support diagnostic and therapeutic practice. Cardiac fluid dynamics represents a challenge in this sense. The visualization of flow in the heart chambers is, in fact, still of little usage in diagnosis.

Left ventricular fluid dynamics has been studied by several authors with particular attention on its filling (diastolic) phase, where the interaction between flow and tissues is found to be relevant in the heart function (Mandinov et al., 2000; Vasan and Levy, 2000). First studies about the flow inside the left ventricle permitted the interpretation of diagnostic images in terms of vortex dynamics (Steen and Steen, 1994; Vierendeels et al., 2002; Baccani et al., 2002) by comparison of the space–time map of the axial velocity with clinical echo-Doppler imaging (transmitral M-mode). These studies were performed using axially symmetric models. The presence of a three-dimensional flow structure was recognized since the early experimental studies (Bellhouse, 1972; Reul et al., 1981; Wieting and Stripling, 1984). They observed that the transmitral jet quickly deforms into an asymmetric vortex wake. The pictures of the flow field typically show a large vortex behind the anterior mitral valve leaflet and a circulatory cell that persists until the systolic ejection. More recent experiments, that used image velocimetry techniques and high-speed cameras (Brucker et al., 2002; Cooke et al., 2004; Cenedese et al., 2005; Akutsu et al., 2005; Pierrakos et al., 2005) have shown quantification capabilities in particular for assessing the impact of prosthetic valves on intraventricular flow.

Experiments are commonly limited to the measurements of flow quantities on single points or two-dimensional sections. To overcome this limitation, three-dimensional

*Corresponding author. Tel.: +39 554796 471; fax: +39 55495 333.
E-mail address: federico.domenichini@unifi.it (F. Domenichini).

0021-9290/$ - see front matter © 2006 Elsevier Ltd. All rights reserved.
doi:10.1016/j.jbiomech.2006.09.024

numerical studies have been developed using various methods (Saber et al., 2001; Lemmon and Yoganathan, 2000) that captured the gross features of the flow. The details of the three-dimensional flow during diastole have been investigated numerically for an ideal left ventricle corresponding to a healthy child (Domenichini et al., 2005). This shows that the vortex ring wake, that develops behind the mitral valve, follows a curved path that turns toward the lateral wall. One side of the ring occupies the center of the cavity and gives rise to the experimentally observed circulation. A study based on the same numerical model has shown that the intraventricular energy dissipation is significantly affected by the vortex flow arrangement (Pedrizzetti and Domenichini, 2005). The numerical results have in common the limitation of considering fixed-open mitral valves, this is still a necessary approximation considering the difficulty to properly address the leaflets dynamics.

Accurate numerical simulations are also limited to values of the parameters that are adequate for healthy and young individuals; in particular an increase in the value of the Reynolds number, see definition below, requires a larger increase (to over cubic power) of the computational resources. Ventricular flow for elder humans, in particular in presence of dilated hearts where the Reynolds number grows two or three times, is still at the edge or beyond the capabilities of current computational power. The flow is expected to loose some of its regularity and develop highly entangled vortex dynamics, possibly some turbulence. This represent an important limitation of numerical studies because the flow structure in large hearts is of particular interest for the diagnostic process as these are commonly found under pathological conditions.

In order to perform an additional step toward the understanding of the intraventricular flow, the present study employs either experimental and numerical approaches in combination. The first objective of this work stands in the physical validation of numerical results. These permit to uncover the three-dimensional flow structure at a level of details that cannot be reached experimentally and visualize what lies behind the experimental results. Finally, after the experiments and calculations have proceeded in parallel and their link is made stronger, the experimental system is employed to extend the analysis to conditions that are beyond the capabilities of direct numerical simulations, where some intraventricular turbulence develops.

2. Definitions and methods

A left ventricle model is represented by an axisymmetric cavity with moving walls. The dynamics of the wall specifies the variation of the ventricular volume $V^*(t^*)$, where the * is used to indicate dimensional variables, and of the entering/exiting discharge $Q^*(t^*) = \mathrm{d}V^*/\mathrm{d}t^*$, that are both periodic with the heartbeat period T.

The inlet and outlet orifices, that represent the mitral and aortic valves, are assumed to be of fixed circular shape. They are contained in the equatorial plane whose end-systolic diameter is indicated with D_0. The diameters of the mitral and aortic orifices are then $\sigma_m D_0$ and $\sigma_a D_0$, where σ_m and σ_a are the dimensionless orifice sizes. Both orifices are aligned along a same equatorial diameter and their positions are specified by the displacements of their centers with respect to the center of the equatorial circle, $\varepsilon_m D_0$ and $\varepsilon_a D_0$, where ε_m and ε_a are dimensionless eccentricities. This arrangement, sketched in Fig. 1a, defines a geometric plane of symmetry that crosses the cavity longitudinally in analogy to the scanplane employed in standard two-dimensional ultrasound imaging.

In order to simplify the comparisons between numerical and experimental results, the problem is made dimensionless assuming D_0 as the unit of length and T as the unit of time. In such a way all the lengths are referred to D_0, times to T, and similarly for all the derived quantities. The dimensionless flow problem is thus characterized by the Stokes parameter $\beta = D_0^2/\nu T$, where ν is the kinematic viscosity, that for the blood is about $\nu = 3 \times 10^{-6}\,\mathrm{m}^2/\mathrm{s}$,

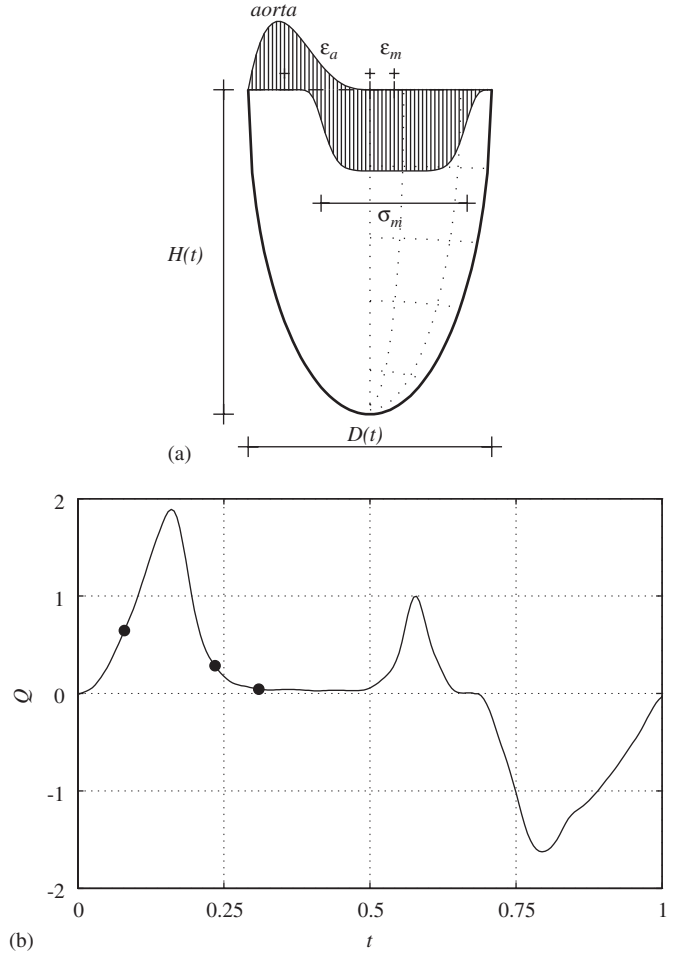

Fig. 1. (a) Sketch of the problem geometry. (b) Time law of the dimensionless discharge $Q(t)$, $St = 0.06$. The markers indicate $t = [10\,30\,40]/128$.

and by the dimensionless description of the wall motion that forces the flow across the valves. The Stokes parameter represents the importance of the viscous diffusion, whose characteristic length is $(\nu T)^{1/2}$, relative to the unit length D_0; at higher values of β the influence of viscosity is reduced and dissipation occurs at smaller scales.

The ventricular wall dynamics is firstly specified by the time profile of the dimensionless discharge $Q(t) = Q^*(Tt)T/D_0^3$, and by the effective chamber geometry expressed in terms relative to the D_0 unit. A standard profile $Q(t)$ is employed in this work, it is selected from a series of recording on healthy individuals, Fig. 1b; positive values correspond to the mitral inflow, negative ones correspond to the aortic outflow. In global terms, the flow can be characterized by a reference velocity V taken as the peak velocity across the mitral valve $V = \max(4Q^*/\pi\sigma_m^2 D_0^2)$, from this a definition for the Strouhal number follows as $St = D_0/VT$. The Strouhal number is the ratio between the unit length and a length which describes the convection of the mitral jet; at lower values of St, the entering jet is expected to penetrate more deeply the cavity. Small healthy hearts are characterized by small values of β and sufficiently high values of St (Pedrizzetti and Domenichini, 2005); dilated adult hearts presents sensibly higher β and smaller St (Lentner, 1990). A Reynolds number can be defined as $Re = VD_0/\nu = St^{-1}\beta$.

2.1. Experimental setup

The experimental setup is sketched in Fig. 2. A model ventricle is placed inside of a $18 \times 18 \times 30$ cm Plexiglas chamber filled with water and connected to a piston-cylinder device. The piston, with diameter 10 cm, is driven by a computer-controlled linear motor (Baldor actuator) able to reproduce any required law of motion. The motion of the piston changes the total volume of the chamber, so that the ventricle increases or reduces its volume accordingly. The model ventricle is made of a transparent, 0.15 cm thick, silicone rubber. At rest it is approximately 8 cm high, the base is a circular Plexiglas plate, diameter 5.6 cm, with two circular orifices, diameters 2.3 cm and 1.7 cm, that model the mitral and aortic openings, respectively. The circuit is closed by two tubes that connect the orifices to a constant head reservoir. Two one-way valves are inserted along such tubes, in order to avoid backflows. The impedance of the circulatory network is simulated by a chamber partially filled with air and by an adjustable resistance placed along the aortic duct.

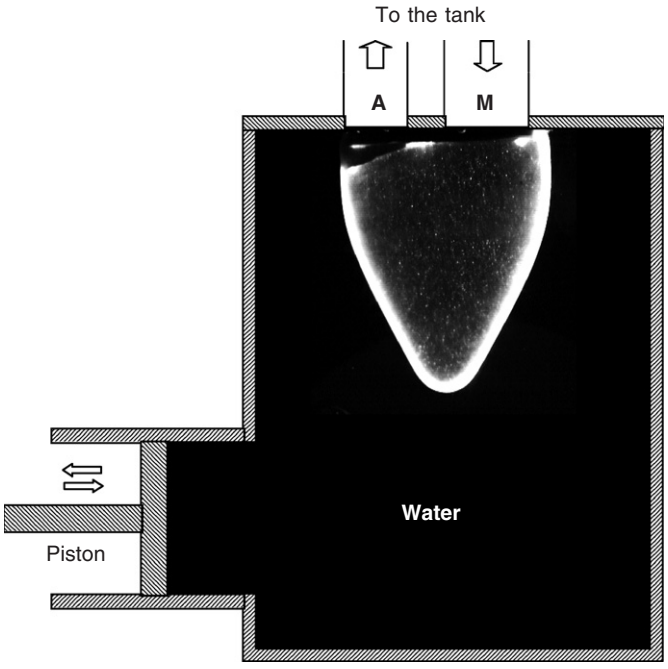

Fig. 2. Sketch of the experimental model ventricle inside the vessel connected to the piston-cylinder device. A and M represent the aortic and mitral opening, respectively.

The slightly enlarged section immediately below the fixed plate is taken as the reference equatorial plane. The minimum diameter D_0 at this level is 6 cm, therefore $\sigma_m = 0.38$ and $\sigma_a = 0.28$. The experiments are performed with a period T of 6 and 12 s, that give $\beta = 600$ and 300, respectively; such values are in the physiological interval that ranges from about 100 in babies to over 500 for old dilated hearts (Lentner, 1990). The time law of $Q(t)$, Fig. 1 is enforced with a stroke volume SV of 32, 48, and 64 cm^3 that is proportional to the reference velocity; the Strouhal number can be rewritten as $St = kD_0^3/\mathrm{SV}$ where the proportionality constant k, that depends on the value of σ_m and on the shape of the profile $Q(t)$, is in this arrangement approximately $k = 0.018$. St varies from 0.06 to 0.12, well into the physiological range that could possibly extend to values slightly smaller than these (Lentner, 1990).

The vertical mid-plane that contains the centers of the inlet and outlet openings is illuminated by an infrared laser sheet (12 W). A high-speed camera is used to acquire series of grayscale images with a resolution of 420×480. The frame rate of 125 or 250 Hz is employed for experiments with $T = 12$ s or $T = 6$ s, respectively.

The two components of the velocity on the scanplane have been estimated by a feature tracking algorithm on a regular 51×51 grid (Cenedese et al., 2005). Typically, 10 cycles have been acquired for each experiment and the average cycle is presented here. The case with $T = 6$ s and SV = 64 cm^3 ($\beta = 600$, $St = 0.06$) shows some relevant turbulence and 100 cycles have been acquired in order to reliably compute second order statistics.

2.2. Numerical setup

The numerical left ventricle (Domenichini et al., 2005) is made of a half prolate spheroid whose moving geometry is described by the equatorial diameter $D(t)$ and the major semi-axis $H(t)$. In order to best approximate the experimental setup, the numerical geometry is obtained from that automatically extracted (thresholding) from the

experimental images. The experimental geometry does not match exactly that of a prolate spheroid, therefore on each instant the values $D(t)$ and $H(t)$ that best approximate the wall are obtained under the constraint that the spheroid volume is identical to the experimental one by a one-dimensional error minimization procedure.

The flow dynamics inside the prolate spheroidal cavity is then computed numerically. The Navier–Stokes equations are written in the moving body-fitted system of orthogonal coordinates with a Fourier representation along the azimuthal direction. These are solved numerically with a mixed finite differences—spectral method (Domenichini and Baccani, 2004; Domenichini et al., 2005). The flow is forced by the known motion of the ventricle wall, i.e. by the functions $D(t)$ and $H(t)$; the time variation of the cavity volume corresponds to the entering/exiting discharge of Fig. 1. Once the instantaneous $Q(t)>0$ is known, a bulk circular velocity profile, of size σ_m and eccentricity ε_m, is imposed at the equatorial plane (Pedrizzetti and Domenichini, 2005); similarly, an exit profile is given when $Q(t)<0$, although the shape of the exiting profile has a little influence on the intraventricular flow. The results here presented have been obtained with a 96×96 grid on the meridian plane and 8 Fourier harmonics.

The numerical study is performed in the same range 0.06–0.12 of the Strouhal number considered in the experiments, the value of the Stokes number is kept fixed to $\beta = 300$. Above such limits the appearance of turbulence requires a substantial increase of the resolution that is not feasible by the available resources or would require a sub-grid scale modeling that is also not available for such highly nonhomogenous fields.

3. Results

The flow found experimentally for $\beta = 300$ and $St = 0.06$ is shown in Fig. 3a–c, where the instantaneous vorticity fields on the plane of symmetry are reported. The corresponding (computed from the in-plane velocity components) numerical fields are reported in Fig. 3d–f. The similarity between experiments and calculations is remarkable despite minor differences in LV geometry and notwithstanding the apparent higher smoothness of the numerical results that are free from measurement noise. At the beginning of diastole, the head of the mitral jet appears as two counter-rotating vortices on the scanplane, Fig. 3a, d. The left vortex moves quickly toward the center of the chamber, Fig. 3b, e, while the right one slows down approaching the ventricle wall; the entering jet is deflected toward the lateral wall (Domenichini et al., 2005). During diastasis, Fig. 3c, f, the vortex structure loses its coherence and develops smaller scales that rapidly dissipate, this is due to the three-dimensional dynamics that is not visible on the symmetry plane.

The numerically computed three-dimensional vortex structure is shown in Fig. 4. The initial vortex ring structure is the head of the entering jet; its central part penetrates more deeply into the cavity producing a tilting of the wake structure. The vortex interacts with the boundary layer at the lateral wall where it is locally

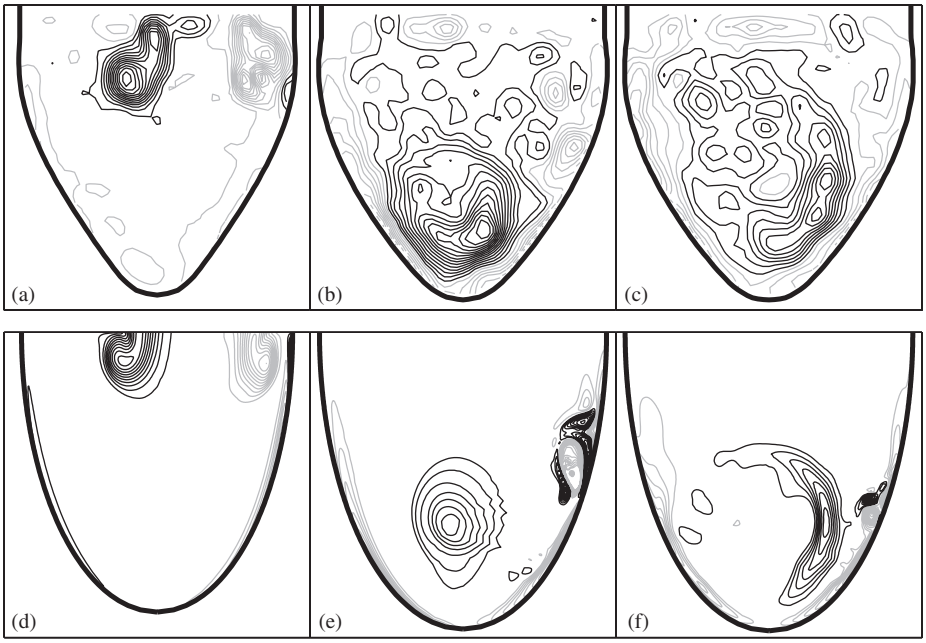

Fig. 3. Experimental (a, b, c) and numerical (d, e, f) results for $\beta = 300$ and $St = 0.06$. Instantaneous vorticity fields (equispaced levels) on the plane of symmetry at $t = [10\,30\,40]/128$. Positive (clockwise) values corresponds to gray lines, negative values to black ones. Vorticity values: (a) from -40 to $50\,s^{-1}$; (b) from -20 to $20\,s^{-1}$; (c) from -15 to $15\,s^{-1}$; (d, e, f) corresponding dimensionless numerical values. Lateral wall and interventricular septum correspond to the right and left sides, respectively.

dissipated. Dissipation rapidly propagates along the vortex and destroys its coherent pattern until, at the end of the diastole (not shown in figure), the wake structure is mostly dissipated. The same dynamics is suggested by the experiments where the vortex rapidly disappears at the end of filling phase. The experimental results correspond to an average over 10 heartbeats, their statistical analysis showed signs of weak turbulence developing during flow deceleration, although its intensity is very small and hardly recognizable from experimental noise.

The influence of a change in the Strouhal number to $St = 0.12$ is shown in Fig. 5. A higher Strouhal number implies the shortening of the jet that enters less in depth into the cavity, the impact of the vortex structure to the wall is substantially reduced as well as the associated dissipation. The three-dimensional vorticity field remains well recognizable at all instants. It shows a weaker interaction with the boundary layer and a less evident deformation until the ejection through the aortic orifice. No sign of turbulence is found. The slightly poorer agreement could be imputable to the possible minor differences in the velocity profile of the mitral jet.

The effect of increasing the value of the Stokes number to $\beta = 600$ and keeping $St = 0.06$ is now analyzed on the

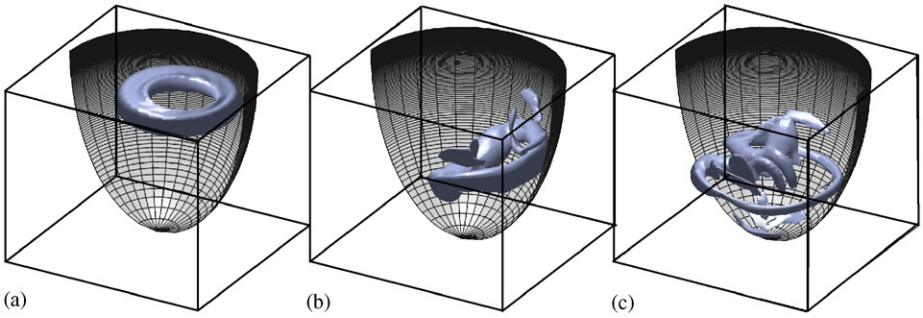

Fig. 4. Numerical results, $\beta = 300$ and $St = 0.06$. The vortex structure is shown as isosurfaces of the λ_2 parameter (Jeong and Hussain, 1995), $\lambda_2 = -1000$, at $t = [10\,30\,40]/128$. Lateral wall and interventricular septum correspond to the right and left sides, respectively.

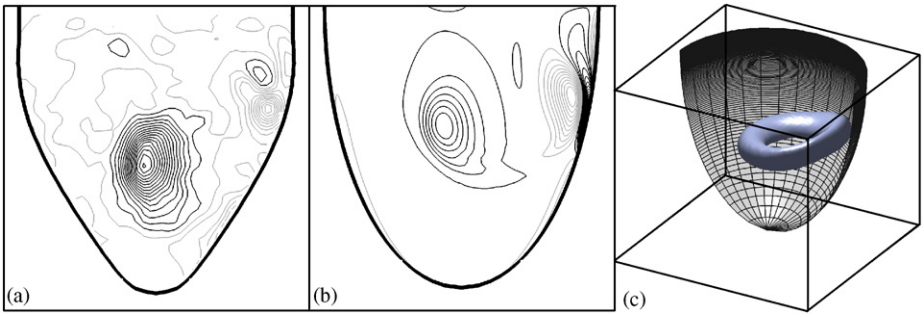

Fig. 5. Results for $\beta = 300$ and $St = 0.12$ at $t = \frac{40}{128}$. Instantaneous experimental (a) and numerical (b) vorticity fields (equispaced levels) on the plane of symmetry. Vorticity values: (a) from -15 to $10\,s^{-1}$, (b) corresponding dimensionless numerical values. Positive (clockwise) values corresponds to gray lines, negative values to black ones. (c) Instantaneous numerical isosurfaces of λ_2 ($\lambda_2 = -100$). Lateral wall and interventricular septum correspond to the right and left sides, respectively.

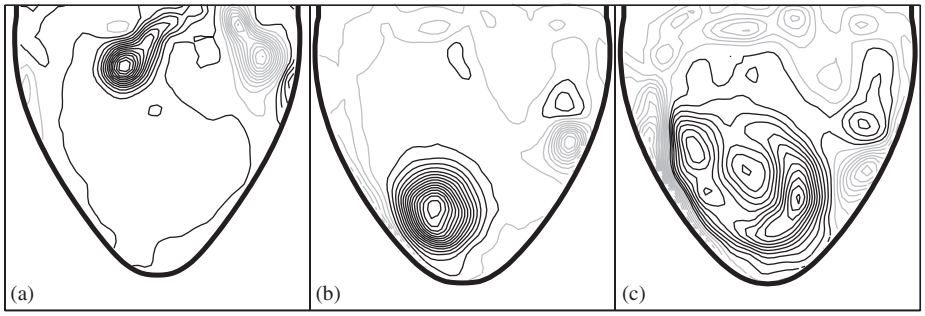

Fig. 6. Experimental results for $\beta = 600$ and $St = 0.06$. Instantaneous vorticity fields (equispaced levels) on the plane of symmetry at $t = [10\,30\,40]/128$. Vorticity values: (a) from -90 to $90\,s^{-1}$, (b) from -60 to $50\,s^{-1}$, (c) from -25 to $30\,s^{-1}$. Positive (clockwise) values corresponds to gray lines, negative values to black ones. Lateral wall and interventricular septum correspond to the right and left sides, respectively.

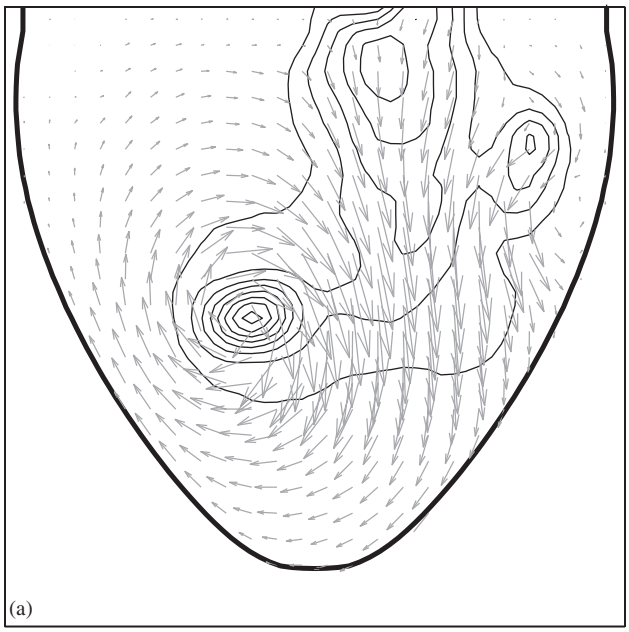

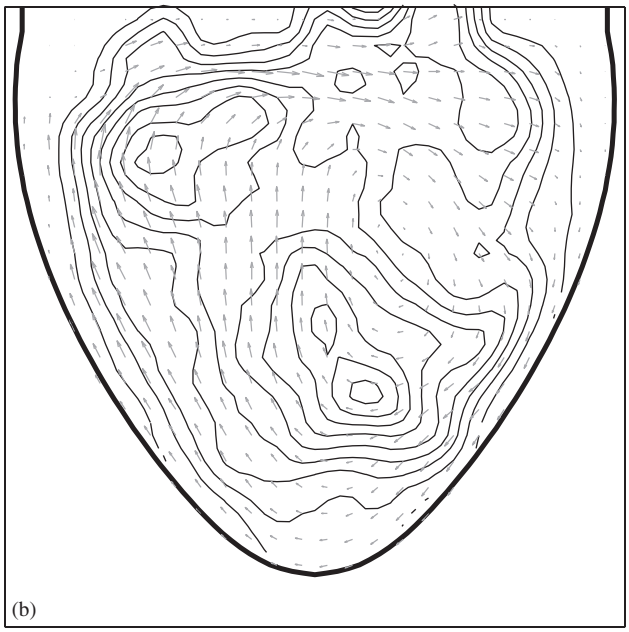

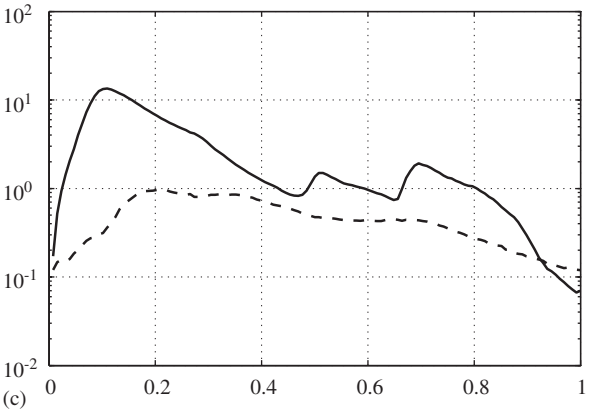

basis of experimental results only. This case, that corresponds to a peak Reynolds number $Re = \beta/St = 10^4$, is out of our available numerical resources. The flow shown in Fig. 6 represents the mean flow obtained by averaging 100 heartbeats. A comparison with Fig. 3 shows that the Stokes parameter has a little influence on the flow pattern; the increase of β corresponds to a reduction of the viscous effects and therefore to the appearance of smaller vorticity structures (although this is not noticeable in the pictures where average flow appears smooth). Changes of the flow evolution cannot be depicted from the average fields here reported, they can be appreciated analyzing the turbulent fluctuations, as discussed below.

The presence of turbulence can be depicted in Fig. 7a, b, where the arrows represents the mean flow and the contour maps the distribution of the in-plane kinetic energy of fluctuations (turbulence). Fluctuations are found in the flow in correspondence of the main vortex structure during the diastolic filling, Fig. 7a, although these may be more imputable to the large gradients and small changes in the vortex trajectory than to turbulence. Significant turbulence develops during the deceleration phase, Fig. 7b, where it is associated with the dissipation of the vortex structure. Turbulence does not affect significantly the mean flow, however it increases energy dissipation and therefore reduces the efficiency of the heart pump. The unsteady development of turbulence can be appreciated in Fig. 7c where the time evolution of the in-plane turbulent kinetic energy is plotted with that of the mean flow. The peak of turbulent energy is found during the deceleration of the E-wave. It is maintained at significant levels during the whole diastasis indicating a continuous production during the vortex dissipation process.

4. Discussion

The fluid dynamics structure that develops into the left ventricle has been analyzed using a combination of experimental and numerical models. The results have shown a good agreement between experiments and calculations, up to a quantitative level, despite some minor differences in the details of the models. This has been shown during diastole, when most flow complexity develops. In general, they have confirmed the known qualitative picture of the flow. It is made of a mitral jet that is deflected toward the lateral wall. The wake vortex structure is that of a ring that on one side interacts with the lateral wall while the other side occupies the cavity center giving rise to a circulatory cell that is eventually dissipated during the following contraction phase (Pedrizzetti and Domenichini, 2005).

Fig. 7. Experimental results for $\beta = 600$ and $St = 0.06$. (a, b). Instantaneous velocity fields (vectors) and distributions of the in-plane turbulent kinetic energy at $t = [20\,55]/128$. Lateral wall and interventricular septum correspond to the right and left sides, respectively. Time evolution (c) of the kinetic energy of mean flow (solid line) and turbulent fluctuations (dashed line).

The intraventricular flow structure depends on two dimensionless parameters: the Stokes number β and the Strouhal number St. The Strouhal number has a fundamental relevance on the flow evolution. Its reciprocal is a measure of the length of the jet: when reducing St, the jet enters more deeply inside the ventricle, up to possibly impacts on the apical wall. The numerical simulations have allowed to understand the three-dimensional structure of the flow. In particular they have shown that, when reducing St, the intraventricular vortex ring undergoes a stronger interaction with the boundary layer at the lateral wall. The local dissipation generates axial flow waves on either side, they eventually collide on the opposite side and produce the degradation of the whole structure. The higher the impact on the lateral wall, the higher is the following dissipation. When β is increased the viscous dissipation occurs at increasingly small scales and, when St is small enough, the mitral jet impacts the apex and turbulence may develop.

It is worth noticing that the agreement between the experimental and computational results, obtained with slightly different shapes of the cavity, suggests that the details of the actual geometry have little influence on the flow dynamics, when the basic parameters are maintained.

The current study neglects some elements of realistic ventricles, in particular the mitral valve is assumed to be fixed open and papillary muscles are not present. Their interaction with the flow represents additional disturbances to the vortex structure and are expected to stimulate the appearance of turbulence, although no indication can be supported about the degree of their influence. The results are also limited to the conditions of healthy ventricles. Pattern modifications in presence of specific pathologies, geometrical remodeling, or flow modifications are still not addressed. These results give some indication about the behavior of the flow structure when basic parameters are changed. These could be of preliminary support in the development of diagnostic indicators based on fluid dynamics.

References

Akutsu, T., Imai, R., Deguchi, Y., 2005. Effect of the flow field of mechanical bileaflet mitral prostheses on valve closing. Journal of Artificial Organs 8, 161–170.

Baccani, B., Domenichini, F., Pedrizzetti, G., Tonti, G., 2002. Fluid dynamics of the left ventricular filling in dilated cardiomyopathy. Journal of Biomechanics 35 (5), 665–671.

Bellhouse, B.J., 1972. Fluid mechanics of a model mitral valve and left ventricle. Cardiovascular Research 6, 199–210.

Brucker, C., Steinseifer, U., Schroder, W., Reul, H., 2002. Unsteady flow through a new mechanical heart valve prosthesis analysed by digital particle image velocimetry. Measurement Science and Technology 13, 1043–1049.

Cenedese, A., Del Prete, Z., Miozzi, M., Querzoli, G., 2005. A laboratory investigation of the flow in the left ventricle of the human heart with prosthetic, tilting-disk valves. Experiments in Fluids 39 (2), 322–335.

Cooke, J., Hertzberg, J., Boardman, M., Shandas, R., 2004. Characterizing vortex ring behaviour during ventricular filling with Doppler echocardiography: an in vitro study. Annals of Biomedical Engineering 32 (2), 245–256.

Domenichini, F., Baccani, B., 2004. A formulation of Navier–Stokes problem in cylindrical coordinates applied to the 3D entry jet in a duct. Journal of Computational Physics 200 (1), 177–191.

Domenichini, F., Pedrizzetti, G., Baccani, B., 2005. Three-dimensional filling flow into a model left ventricle. Journal of Fluid Mechanics 539, 179–198.

Jeong, J., Hussain, F., 1995. On the identification of a vortex. Journal of Fluid Mechanics 285, 69–94.

Lemmon, J.D., Yoganathan, A.P., 2000. Computational modeling of left heart diastolic function: examination of ventricular dysfunction. Journal of Biomechanical Engineering 122, 297–303.

Lentner, C. (Ed.), 1990. Geigy Scientific Tables, Vol. 5: Heart and Circulation, eighth ed., Ciba-Geigy Limited, Basel, Switzerland.

Mandinov, L., Eberli, F.R., Seiler, C., Hess, O.M., 2000. Review: diastolic heart failure. Cardiovascular Research 45, 813–825.

Pedrizzetti, G., Domenichini, F., 2005. Nature optimizes the swirling flow in the human left ventricle. Physical Review Letters 95, 1080101.

Pierrakos, O., Vlachos, P.P., Telionis, D.P., 2005. Time-Resolved DPIV analysis of vortex dynamics in a left ventricular model through bileaflet mechanical and porcine heart valve prostheses. Journal of Biomechanical Engineering 126 (6), 714–726.

Reul, H., Talukder, N., Muller, W., 1981. Fluid mechanics of the natural mitral valve. Journal of Biomechanics 14 (5), 361–372.

Saber, N.R., Gosman, A.D., Wood, N.B., Kilner, P.J., Charrier, C.L., Firmin, D.N., 2001. Computational flow modeling of the left ventricle based on in vivo MRI data: initial experience. Annals of Biomedical Engineering 29, 275–283.

Steen, T., Steen, S., 1994. Filling of a model left ventricle studied by colour M mode Doppler. Cardiovascular Research 28, 1821–1827.

Vasan, R.S., Levy, D., 2000. Defining diastolic heart failure. Circulation 101, 2118–2121.

Vierendeels, J.A., Dick, E., Verdonck, P.R., 2002. Hydrodynamics of color M-mode Doppler flow wave propagation velocity $V(p)$: a computer study. Journal of the American Society of Echocardiography 15, 219–224.

Wieting, D.W., Stripling, T.E., 1984. Dynamics and fluid dynamics of the mitral valve. In: Duran, C., Angell, W.W., Johnson, A.D., Oury, J.H. (Eds.), Recent Progress in Mitral Valve Disease. Butterworths Publishers, London, pp. 13–46.